Lyman-alpha Solar Telescope (LST) User Guide

Li Feng (lfeng@pmo.ac.cn), Ying Li, Hui Li, Qingmin Zhang
and LST team

Document revision history

	version	revision date	revision description	revision tracking notes
1	1.0	June 25, 2023	user guide created	

Contents

1. LST OVERVIEW 3

1.1 LST INSTRUMENTS 3
1.2 LST SCIENTIFIC OBJECTIVES 4

2. LST DATA PRODUCTS 4

2.1 DEFINITION OF DATA LEVELS 4
2.2 DATA IN DIFFERENT OBSERVING MODES 5
2.3 FIELD OF VIEW (FOV) OF SDI 6
2.4 SDI AND WST DATA DURING EARTH ECLIPSE 7
2.5 KNOWN INSTRUMENTAL ARTIFACTS 7
2.6 FUTURE PRODUCTS 8

3. DATA DOWNLOAD 9

4. SEARCH EVENTS 11

4.1 DAILY MOVIE 11
4.2 IMAGE BROWSER 11
4.3 EVENT LISTS 12

5. DATA ANALYSIS 13

5.1 TWO MAIN DATA ANALYSIS ROUTINES: READ_LST AND LST_PREP 13
5.2 SDI DATA ANALYSIS DEMO 13
5.2.1 SDI cutout data *14*
5.2.2 SDI full-FOV data *14*
5.3 WST DATA ANALYSIS DEMO 16

6. REFERENCES 16

1. LST overview

1.1 LST instruments

The Lyman-alpha Solar Telescope (LST) is one of the three payloads aboard the Advanced Space-based Solar Observatory (Gan et al., 2023). It is composed of a Solar Disk Imager (SDI), a Solar Corona Imager (SCI), a White-light Solar Telescope (WST), and two Guide Telescopes (Li et al., 2019, Chen et al., 2019, Feng et al.,2019). The characteristic parameters of each instrument are listed in Table 1.

Table 1: Characteristic parameters of LST instruments.

parameters	WST	SDI	SCIUV	SCIWL
waveband	360±2 nm	121.6±4.5 nm	122.6±3 nm	700±32 nm
aperture	130 mm	60 mm	60 mm	
FOV	0 – 1.2 Rs	0 – 1.2 Rs	1.1 - 2.5 Rs	1.1 - 2.5 Rs
Image size	4608×4608	4608×4608	2048×2048	2048×2048
cadence	routine (2 min) burst (1 s & 2 s / 5 s) user defined	routine (1 min) burst (a few s/15 s) user defined	~60 s	30-60 s

SDI is to image the Sun from the disk center to 1.2 solar radii in the Lyman-alpha (Lyα) waveband (121.6±4.5 nm) with a cadence of 4 – 60 s. A piezoelectric image stabilization system is adopted for both SDI and SCI. WST is designed to image the Sun in violet narrow-band continuum (360±2 nm) from the disk center to 1.2 solar radii with a cadence of 1 – 120 s (it can be as high as 0.2 s in the burst mode). A 4608 by 4608 CMOS sensor is selected to be the detector for both SDI and WST, which allows a windowed observation mode with higher time cadence in the burst mode. Since the launch of ASO-S, SDI and WST have been working almost normally. However, the spatial resolution is lower than the designed value of 1.2 arcsec.

SCI is to image the inner solar corona from 1.1 to 2.5 solar radii with a cadence of 3 – 60 s in both Lyα (122.6±3 nm) and white-light (700±32 nm). A beam-splitter divides the coming coronal light into two beams: the reflected beam feeds the Lyα channel while the transmitted beam feeds the white-light channel. The Lyα channel consists of a Lyα filter and a detector; the white-light channel consists of a broadband filter centered at 700 nm, linear polarizers and a detector. Three linear polarizer orientations

(0, ±60°) are used to conduct the polarization measurement in the white-light waveband. In orbit SCI does not work as expected. However, it can sometimes observe eruptive prominences and coronal mass ejections (CMEs) in Lyα and white-light.

1.2 LST scientific objectives

– What is the relationship between solar flares, CMEs and eruptive prominences?
– What triggers solar flares and CMEs, and how do their parameters evolve during the eruptive process?
– What are the physical properties and processes of white-light flares (WLFs)?
– What are the acceleration mechanisms of CMEs in the inner corona? What are their kinetic behaviors?
– How are shock waves formed and what favors the acceleration of solar energetic particles (SEPs) by shock waves?

2. LST data products

2.1 Definition of data levels

The definition of different data levels is shown in Table 2. For SDI and WST, the highest data level is level 2.5. For SCI, the highest data level is level 3.5. At present, level 1 data of SDI and WST have been released. Most of the data calibrations are performed from level 0 to level 1 including dark current, flat field and merging high-gain and low-gain images. The radiometric calibration is done for level 2 data. Note that the radiometric calibration factor for SDI is preliminary, for reference only. For the white-light channel of SCI, polarization calibration is done for level 3.5 data. From level 1 to 1.5 or level 2 to 2.5, anomalous pixel correction and image registration are performed. More details on the LST data products can be found in Feng et al. (2019) with some updates introduced in this user guide.

Table 2: Definition of LST data levels

Level 0	unpacking, verification, adding keywords, etc.
Level 1 **unit: DN**	correcting dark current and flat field, merging high-gain and low-gain images to obtain high-dynamic-range (HDR) images (N/A for WST), indexing bad/missing/spike pixels;
Level 1.5 **unit: DN**	correcting bad/missing/spike pixels, image registration (rotation, translation, scaling);

Level 2 **unit: erg s^{-1} cm^{-2} sr^{-1} or MSB (mean solar brightness)**	radiometric calibration;
Level 2.5 **unit: erg s^{-1} cm^{-2} sr^{-1} or MSB**	correcting bad/missing/spike pixels; image registration (rotation, translation, scaling)
Level 3.5 **unit: MSB**	only for SCIWL total brightness, polarized brightness, etc
quicklook	JPG images

For SDI level 1 data, high-gain & low-gain images taken by the CMOS are merged. It is especially useful for dealing with the saturated regions when large flares occur. The saturated pixels in the high-gain image are replaced by the un-saturated pixels in the low-gain image. In Figure 1, an example is shown for an X-class flare on Jan 9 2023. We can see that the merged image keeps the unsaturated flaring region in the low-gain channel and the unsaturated region in the high-gain channel.

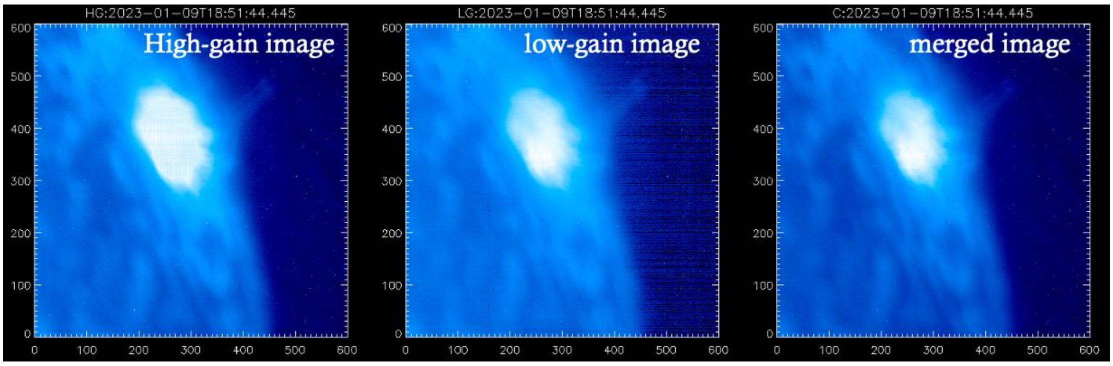

Figure 1 An example shows the merged image from high-gain and low-gain channels for an X-class flare on Jan 9 2023.

2.2 Data in different Observing modes

LST instruments have three modes including routine, burst and user-defined modes. Currently, SDI data in both routine and burst modes are available which have cadences of 1 minute and a few seconds, respectively. When SDI entering the burst mode triggered by the SDI onboard flare triggering software, the observation of 1024*1024 windowed size with a much higher cadence of 4 seconds at the moment is in operation, while the full-disk imaging still runs about every one minute. The position of the SDI window is designed to be transmitted to WST for higher-cadence observations with a cadence of 1 or 2 seconds. This function is still under test. In Figure 2, the full-disk image and the corresponding windowed observation are shown in the left and right panels, respectively. A detailed description of the triggering algorithms of LST can be found in Lu et al. (2020).

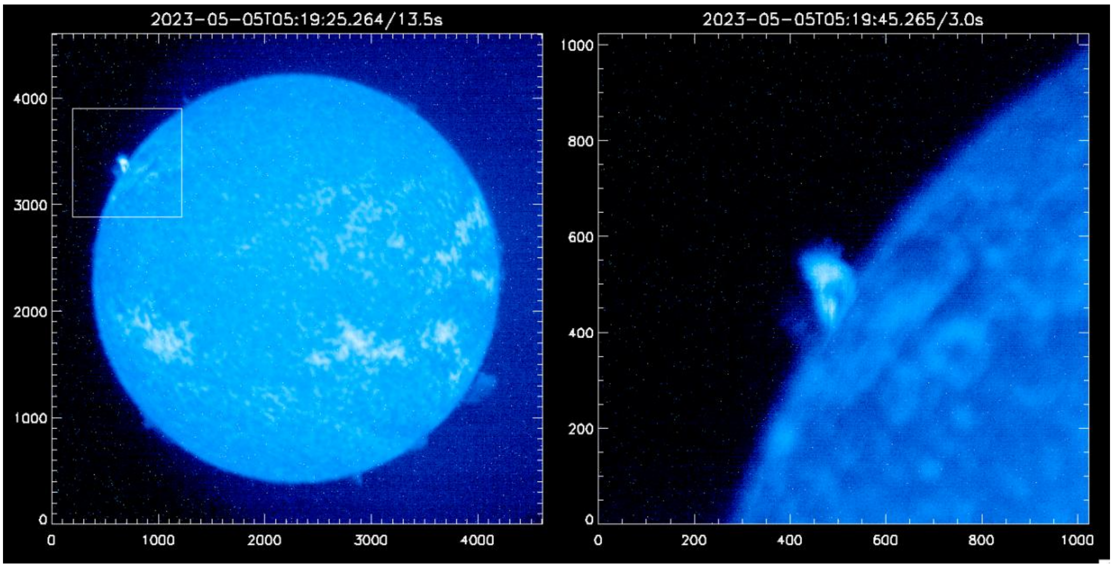

Figure 2 An example of the full-disk image (left) and the corresponding windowed observation of 1024*1024 size (right).

2.3 Field of view (FOV) of SDI

FOV of SDI can be better checked with the flat field image. Details on how to obtain the flat field of SDI using the KLL method can be found in Li et al. (2021). We marked the effective area of the flat field with the red dotted line in Figure 3 which is a circle with a radius of 1.34 Rs centered at (2220, 2563) in the pixel coordinate. It also defines the effective FOV of SDI.

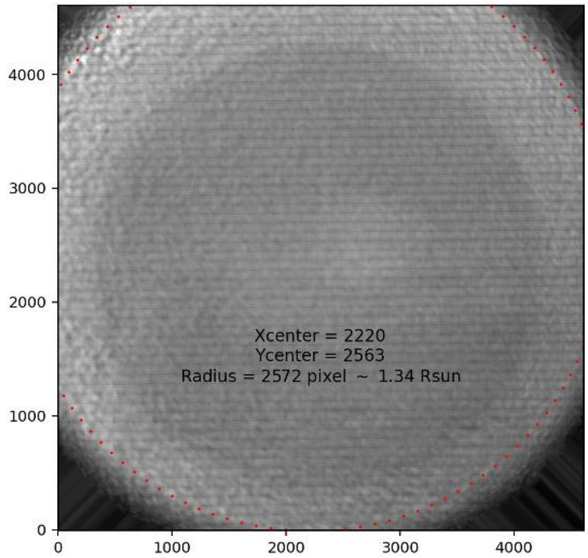

Figure 3 An example of the flat field of SDI with the effective field of view marked by the red dotted line.

2.4 SDI and WST data during earth eclipse

ASO-S has a Sun-synchronous orbit which has very inclined polar orbit with respect to the earth equator. From May to August, when the spacecraft is close to or in the phase of earth eclipse, the absorption of UV emission by the earth atmosphere, or the block of UV emission by the solid earth can be seen. In Figure 4, the SDI (top) and WST (bottom) images around the earth eclipse time period on Jun 22 2023 are illustrated.

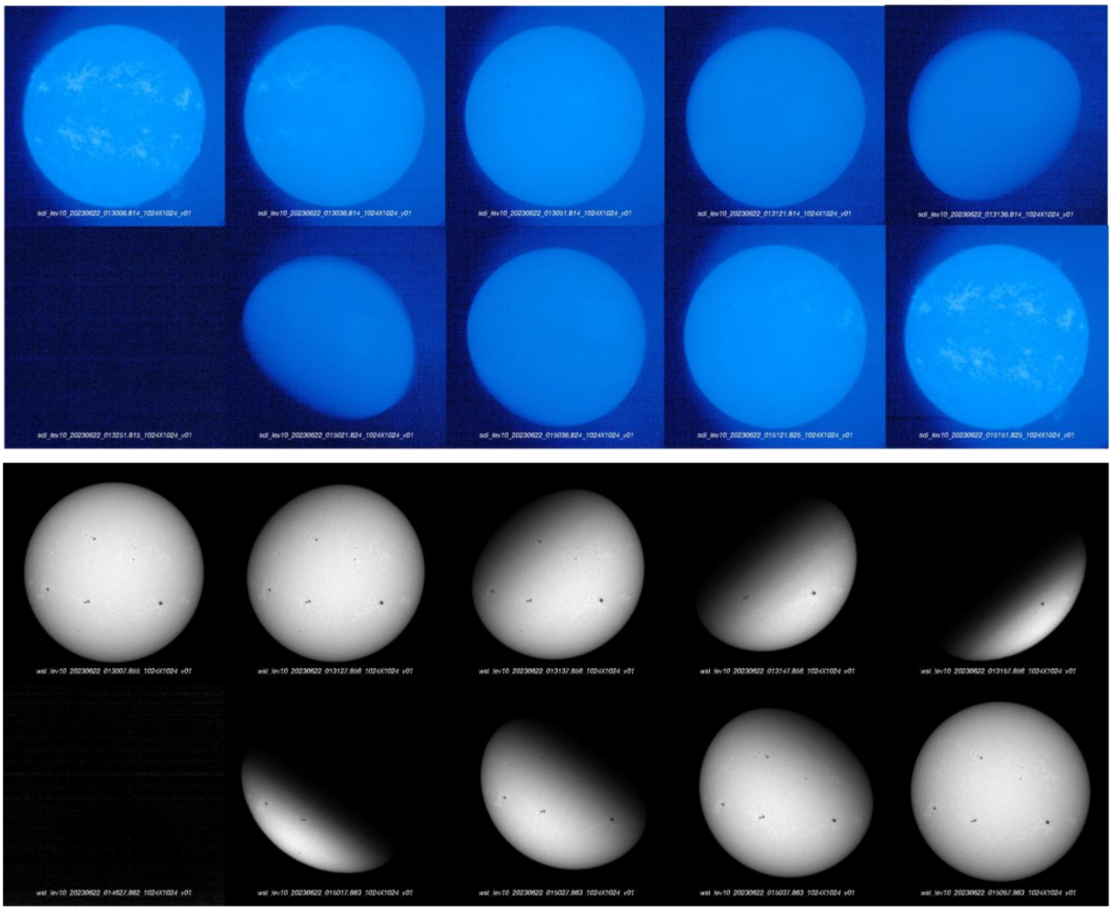

Figure 4 SDI (top) and WST (bottom) images around the earth eclipse time period on Jun 22 2023.

2.5 Known instrumental artifacts

Due to the imperfection of some optical elements of SDI and WST, there are a few known instrumental artifacts that need to be noted. When a rapid brightening spot occurs on the Sun, SDI images it with some unwanted extra surrounding structures (See a SDI subregion in Figure 5a and a simultaneous AIA subregion at 30.4 nm in Figure 5b). For strong white-light flares, there are extra horns due to the imperfect manufacturing of the reflective mirror in the WST image (Figure 5c). For SDI, in addition, the east-west asymmetry beyond the limb is visible as seen in Figure 5d. It is due to the asymmetry of the mirror manufacturing. Such asymmetry can be reduced by subtracting a minimum background accumulated for weeks.

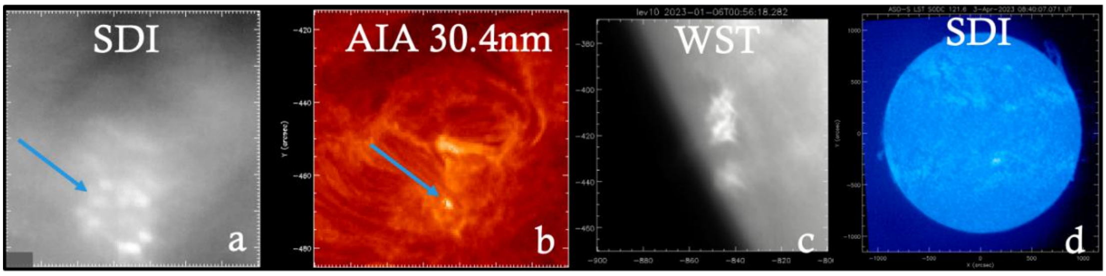

Figure 5 Known SDI and WST instrumental artifacts.

2.6 Future products

Some further data products are still under development. For example, the summary file (Figure 6) of the level 1 data including the key fits header values can be used for statistics. It is organized monthly. The SDI synoptic map (Figure 7) is useful as it provides the incident emission of Lyα in the coronagraph FOV.

lst > summary > lev10 > 2023 > sdi_lev10_202306_summary_v10.txt

FileName	DateObs	Polar	Xsize	Ysize	Exptime	DataMean	DataMedn	DataTot	ObsMode	SAA	Quality
sdi_lev10_20230601_000002.658_v01.fits.gz	2023-06-01T00:00:02	121.6	1024	1024	3.00	92.43	90.21	9.6922e+07	burst	F	0
sdi_lev10_20230601_000006.658_v01.fits.gz	2023-06-01T00:00:06	121.6	1024	1024	3.00	90.57	88.15	9.4968e+07	burst	F	0
sdi_lev10_20230601_000010.658_v01.fits.gz	2023-06-01T00:00:10	121.6	1024	1024	3.29	100.77	98.77	1.0566e+08	burst	F	0
sdi_lev10_20230601_000014.658_v01.fits.gz	2023-06-01T00:00:14	121.6	1024	1024	3.50	106.31	104.30	1.1148e+08	burst	F	0
sdi_lev10_20230601_000018.658_v01.fits.gz	2023-06-01T00:00:18	121.6	1024	1024	3.50	106.80	104.81	1.1199e+08	burst	F	0
sdi_lev10_20230601_000022.658_v01.fits.gz	2023-06-01T00:00:22	121.6	1024	1024	3.50	105.60	103.47	1.1073e+08	burst	F	0
sdi_lev10_20230601_000026.658_v01.fits.gz	2023-06-01T00:00:26	121.6	1024	1024	3.50	106.93	104.77	1.1213e+08	burst	F	0
sdi_lev10_20230601_000030.658_v01.fits.gz	2023-06-01T00:00:30	121.6	1024	1024	3.50	106.36	104.28	1.1152e+08	burst	F	0
sdi_lev10_20230601_000034.658_v01.fits.gz	2023-06-01T00:00:34	121.6	1024	1024	3.50	106.34	104.10	1.1150e+08	burst	F	0
sdi_lev10_20230601_000038.658_v01.fits.gz	2023-06-01T00:00:38	121.6	1024	1024	3.50	106.66	104.66	1.1184e+08	burst	F	0
sdi_lev10_20230601_000042.658_v01.fits.gz	2023-06-01T00:00:42	121.6	1024	1024	3.50	106.79	104.85	1.1198e+08	burst	F	0
sdi_lev10_20230601_000046.658_v01.fits.gz	2023-06-01T00:00:46	121.6	1024	1024	3.50	107.26	105.29	1.1247e+08	burst	F	0
sdi_lev10_20230601_000050.658_v01.fits.gz	2023-06-01T00:00:50	121.6	1024	1024	3.50	106.71	104.77	1.1190e+08	burst	F	0
sdi_lev10_20230601_000054.658_v01.fits.gz	2023-06-01T00:00:54	121.6	1024	1024	3.50	106.74	104.67	1.1193e+08	burst	F	0
sdi_lev10_20230601_000058.658_v01.fits.gz	2023-06-01T00:00:58	121.6	1024	1024	3.50	106.94	104.94	1.1214e+08	burst	F	0
sdi_lev10_20230601_000102.658_v01.fits.gz	2023-06-01T00:01:02	121.6	1024	1024	3.50	106.92	104.81	1.1212e+08	burst	F	0
sdi_lev10_20230601_000106.658_v01.fits.gz	2023-06-01T00:01:06	121.6	1024	1024	3.50	105.98	104.17	1.1112e+08	burst	F	0
sdi_lev10_20230601_000111.658_v01.fits.gz	2023-06-01T00:01:11	121.6	4608	4608	13.50	315.59	348.36	6.7011e+09	burst	F	0
sdi_lev10_20230601_000131.658_v01.fits.gz	2023-06-01T00:01:31	121.6	1024	1024	3.50	107.14	104.89	1.1234e+08	burst	F	0
sdi_lev10_20230601_000135.659_v01.fits.gz	2023-06-01T00:01:35	121.6	1024	1024	3.50	107.20	104.84	1.1241e+08	burst	F	0
sdi_lev10_20230601_000139.659_v01.fits.gz	2023-06-01T00:01:39	121.6	1024	1024	3.50	107.14	104.84	1.1234e+08	burst	F	0
sdi_lev10_20230601_000143.659_v01.fits.gz	2023-06-01T00:01:43	121.6	1024	1024	3.50	106.79	104.58	1.1198e+08	burst	F	0
sdi_lev10_20230601_000147.659_v01.fits.gz	2023-06-01T00:01:47	121.6	1024	1024	3.50	106.26	103.79	1.1142e+08	burst	F	0
sdi_lev10_20230601_000151.659_v01.fits.gz	2023-06-01T00:01:51	121.6	1024	1024	3.50	106.19	103.83	1.1135e+08	burst	F	0
sdi_lev10_20230601_000155.659_v01.fits.gz	2023-06-01T00:01:55	121.6	1024	1024	3.50	107.33	104.89	1.1254e+08	burst	F	0

Figure 6 A snapshot of the SDI summary file for June 2023.

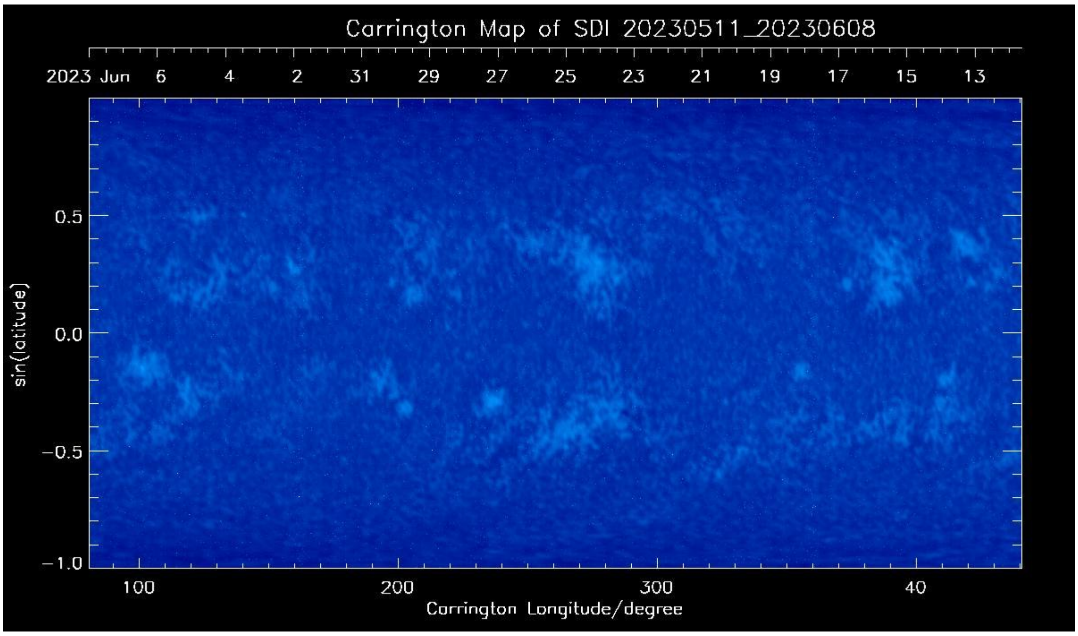

Figure 7 The Carrington map built with the SDI data from May 11 to Jun 8 2023 (Li et al., 2023, in prep).

3. Data download

There are two methods of the LST data download. One is to download the data from the Data Archive webpage (http://aso-s.pmo.ac.cn/sodc/dataArchive.jsp). When users deal with the data in a long time period and are only interested in the data in a fraction of the solar disk, the cutout service is recommended for the data download (http://aso-s.pmo.ac.cn/sodc/cutout.jsp). In Figure 8, a snapshot of the SDI data download via the Data Archive webpage is shown. In Figure 9, a snapshot of the SDI data download with user-defined region of interests via the cutout service is presented.

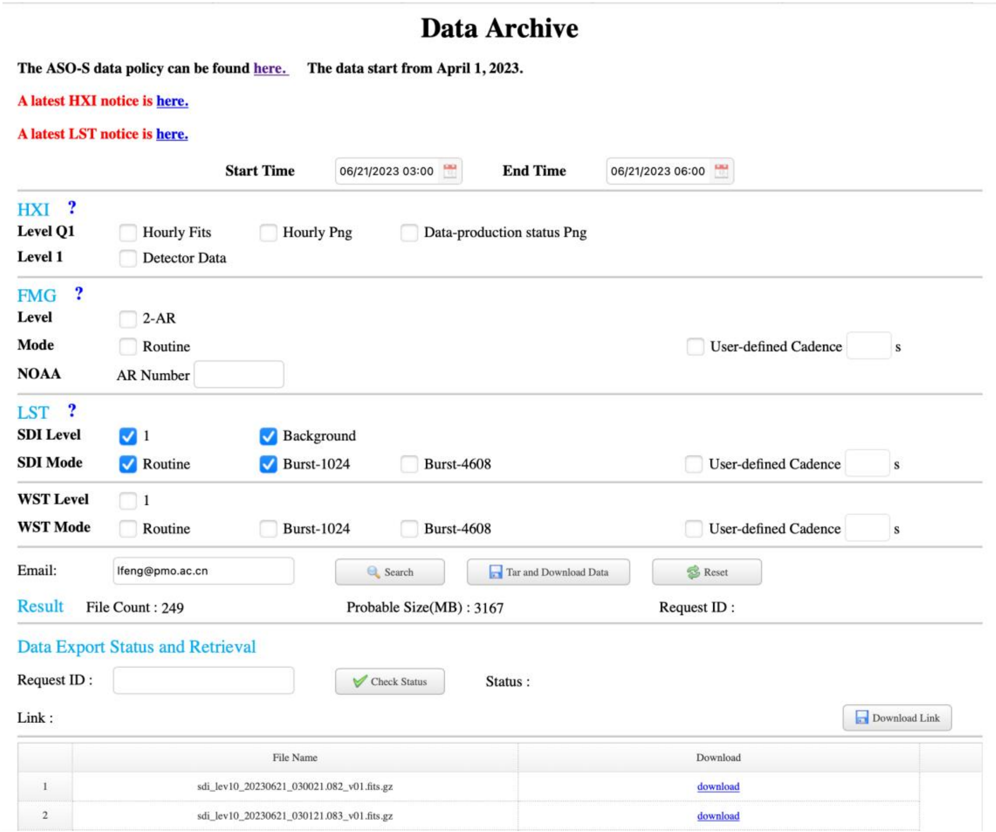

Figure 8 A snapshot of the SDI data download via the Data Archive webpage.

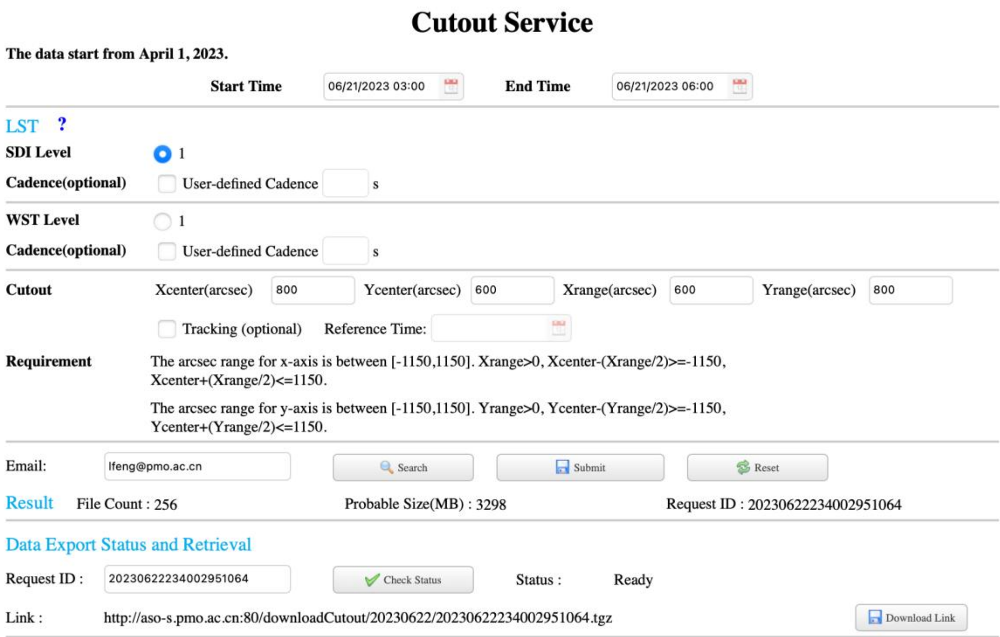

Figure 9 A snapshot of the SDI data download with user-defined region of interests via the cutout service.

4. Search events

To facilitate the search of interested events for users, we designed a few web tools. They are daily movie webpage (http://aso-s.pmo.ac.cn/sodc/asos.jsp) , data browser webpage (http://aso-s.pmo.ac.cn/sodc/imageBrowser.jsp) , and event list webpage (under construction).

4.1 Daily movie

When users input the date, the corresponding SDI and WST daily movies can be viewed and downloaded (Figure 10).

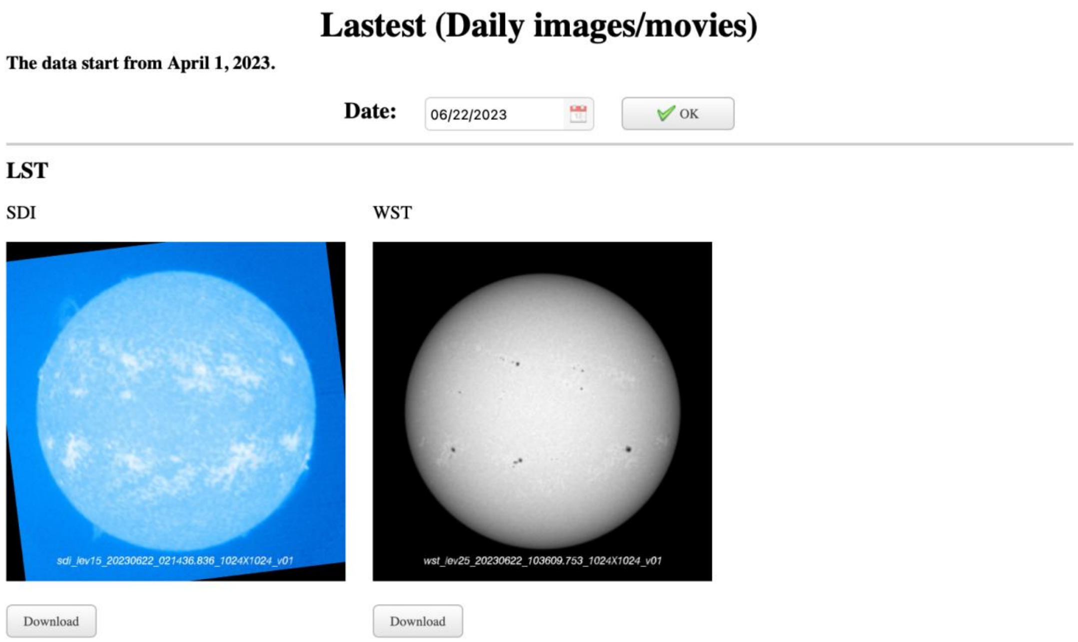

Figure 10 A snapshot of SDI and WST daily movie webpage

4.2 Image browser

The image browser is a useful tool to check the quicklook images of each data with solar north rotated to the image north. Users can choose the cadence, time interval, and different play modes of the slideshow (Figure 11).

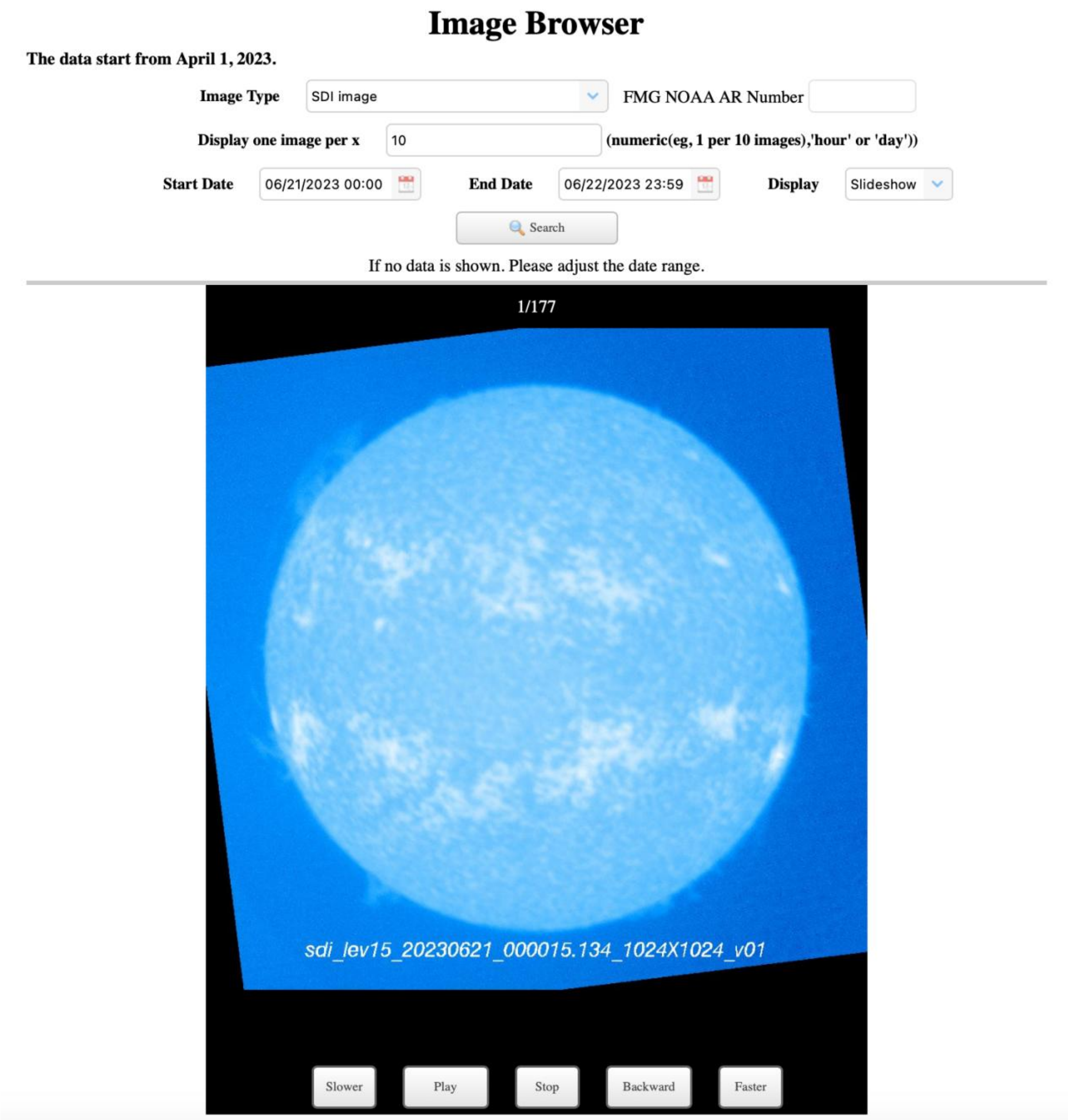

Figure 11 A snapshot of the image browser webpage showing the SDI quicklook image.

4.3 Event lists

Event lists, e.g., flare list, are also planned and the webpage is under construction. An automatic flare detection algorithm is devised. A snapshot of the flare list is demonstrated in the left panel of Figure 12 including the start, end times, duration, position, intensity enhancement (significance), GOES SXR class, and WST flare or not. For each flare, light curves in different wavebands or energy bands observed by ASO-S/HXI, SDI, GOES SXR or its derivative are displayed in the right panel of Figure 12. The SDI image and the zoom-in of the flare region is shown at the bottom.

```
# N:       flare number
# DATE:    day of observation
# START:   start time, earliest indication of detection
# END:     end time, last indication of detection
# DUR:     duration of event in unit of minute
# Xpos:    pixel coordinates along horizontal (X) axis
# Ypos:    pixel coordinates along vertical (Y) axis
# Fpos:    heliographic coordinates of flare position
# SIGN:    maximum intensity increase relative to the background, in %
# CLASS:   the GOES class of the SXR flare
```

N	DATE	START	END	DUR(m)	Xpos	Ypos	Fpos	SIGN(%)	GOES-CLASS	WST-flare
1	2022-12-09	12:39:12	12:57:12	18.0	2240	1856	S13E02	2.8	C4.1	
2	2022-12-09	13:26:12	13:40:12	14.0	4032	3136	N25W78	1.0		
3	2022-12-09	13:50:12	14:16:12	26.0	4032	3136	N25W78	1.5	C3.9	
4	2022-12-09	18:02:12	18:06:12	4.0	4032	3264	N29W90	0.9	C1.5	
5	2022-12-09	22:41:12	23:13:12	32.0	2112	1856	S13E06	3.5	C5.0	
6	2022-12-10	01:14:12	01:45:12	31.0	1984	1472	S25E10	3.0	C1.3	
7	2022-12-10	02:50:12	03:25:12	35.0	1984	1856	S13E10	2.6		
8	2022-12-10	10:21:12	10:37:12	16.0	1856	1344	S30E15	1.6	C4.7	
9	2022-12-10	18:38:12	18:41:12	3.0	1088	2624	N09E39	1.0		
10	2022-12-10	20:15:12	20:27:12	12.0	832	2624	N09E50	0.8	C1.4	
11	2022-12-10	20:40:12	21:03:12	23.0	1728	1344	S30E20	2.9	C4.8	
12	2022-12-11	01:13:12	01:34:12	21.0	1472	1728	S17E27	1.0		
13	2022-12-11	09:13:12	09:26:12	13.0	576	1344	S29E90	8.2		
14	2022-12-11	11:30:12	11:52:12	22.0	576	2496	N05E63	7.2	C2.9	
15	2022-12-11	15:46:12	15:49:12	3.0	576	2624	N09E64	1.2	C1.2	
16	2022-12-12	00:55:12	00:59:12	4.0	576	2496	N05E63	1.3	C3.2	
17	2022-12-12	08:11:12	08:15:12	4.0	448	2496	N05E73	0.8		
18	2022-12-12	09:24:12	09:29:12	5.0	960	1216	S34E56	1.8	C2.1	
19	2022-12-12	15:05:12	15:20:12	15.0	3008	2880	N17W22	2.0	C3.0	
20	2022-12-13	01:43:12	01:47:12	4.0	2240	1472	S26E02	0.5	C1.4	
21	2022-12-13	05:40:12	05:58:12	18.0	2624	2752	N13W10	2.2		
22	2022-12-13	19:49:12	19:53:12	4.0	448	2624	N09E75	1.6		
23	2022-12-13	23:17:12	23:56:12	39.0	448	2624	N09E75	6.4	C2.9	
24	2022-12-14	05:40:12	05:44:12	4.0	1088	2880	N17E40	0.7		
25	2022-12-14	07:33:12	07:55:12	22.0	1088	2752	N13E40	3.4	M2.4	
26	2022-12-14	21:35:12	22:34:12	59.0	832	2752	N13E51	8.6	M4.5	yes
27	2022-12-14	23:44:12	23:48:12	4.0	960	2880	N17E46	1.4	C7.3	
28	2022-12-15	01:35:12	01:40:12	5.0	704	2752	N13E57	2.4	M1.6	
29	2022-12-15	03:05:12	03:10:12	5.0	2752	3008	N20W14	1.4	C4.2	
30	2022-12-15	05:21:12	05:41:12	20.0	832	2752	N13E51	1.4	C7.6	
31	2022-12-15	06:58:12	07:19:12	21.0	832	2880	N17E52	3.9	M2.3	
32	2022-12-15	07:56:12	08:28:12	32.0	832	2752	N13E51	2.7	M1.0	

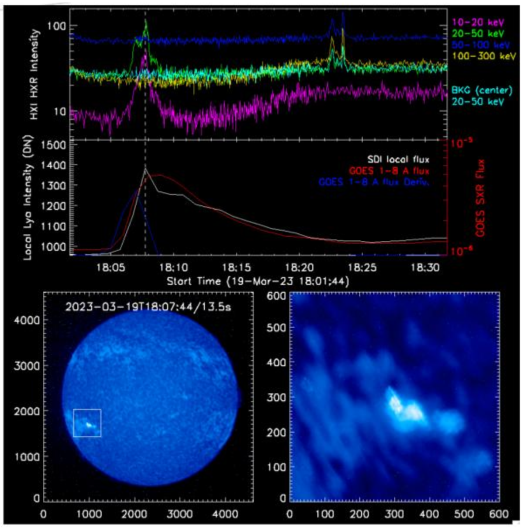

Figure 12 A snapshot of the flare list (left); An example of the details of lightcurves and images for a detected flare (right).

5. Data analysis

5.1 Two main data analysis routines: read_lst and lst_prep

We try to keep the LST data analysis tools as simple as possible. Therefore, users basically only need to invoke read_lst.pro to read the WST or SDI level 1 data, and then use lst_prep.pro to preprocess the level 1 data to higher levels. At the moment, the data analysis tools are written in IDL and have been tested on the Linux, Mac, and Windows operating systems. Users can access the ASO-S data analysis tools via the SolarSoftWare by updating sswidl using:
IDL>ssw_upgrade, /lst,/fmg,/hxi,/loud,/spawnit
An alternative approach is to download the tools via the link below:
http://aso-s.pmo.ac.cn/sodc/analysisSoftware.jsp

The basic usage of the LST data analysis routines is shown below, where ‘fn’ is the filename (including its folder name) of the level 1 fits file.
IDL> read_lst, fn, ihdr, iimg
IDL> lst_prep, ihdr, iimg, ohdr, oimg

5.2 SDI data analysis demo

In this subsection, we demonstrate how to read and preprocess the SDI cutout data and level 1 data. Because of the contamination control, the working temperature of the SDI CMOS is higher than its optimal value. It leads to higher thermal noise in the image. Therefore, we recommend users to add ‘/despike_on’ when using lst_prep.pro. If users deal with only a fraction of the full-FOV data, cutout data is recommended. If a majority of the full FOV with observations beyond the solar limb is used, the normal full-FOV level 1 data is suggested.

5.2.1 SDI cutout data

```
fns=file_search('~/cutout/flare/sdi_lev10_20230403_030*cut.fits.gz')
read_lst, fns, ihdr, iimg ;dealing with a sequence of fits files
lst_prep, ihdr, iimg, ohdr1, oimg1, /despike_on, /la_cosmic, /reg_off
lst_prep, ihdr, iimg, ohdr2, oimg2, /reg_off
index2map, ohdr1[0], oimg1[*,*,0], sdimap1
index2map, ohdr2[0], oimg2[*,*,0], sdimap2
window, 0, xsize=1600, ysize=800, retain=2
!p.multi=[0,2,1]
lst_lct, wavelnth = 1216, instr = 'sdi', /load
plot_map, sdimap1, /log, dmin=20, dmax=14000, charsize=2.
plot_map, sdimap2, /log, dmin=20, dmax=14000, charsize=2.
```

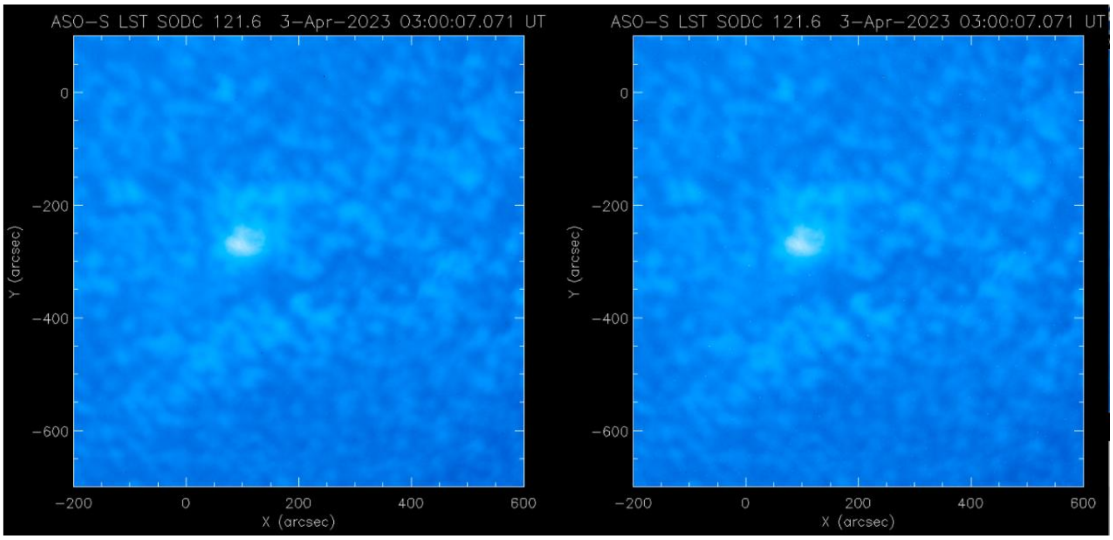

5.2.2 SDI full-FOV data

```
file='/asos/data/sdi/science/lev10/2023/04/03/sdi_lev10_20230403_084007.071_v01.fits.gz'
read_lst, file, ihdr, iimg
bkgfits = '/asos/data/sdi/bkg/2023/sdi_lev10_20230403_bkg_biweekly.fits.gz'
read_lst, bkgfits, bkg_hdr, bkg_dat ;for reducing the east-west asymmetry beyond the limb
lst_prep, ihdr, iimg, ohdr, oimg, /bkgimg_on, bkg_hdr=bkg_hdr, bkg_dat=bkg_dat, /despike_on
index2map, ohdr, oimg, sdimap
window, 0, xsize=1600, ysize=800, retain=2
!p.multi=[0,2,1]
lst_lct, wavelnth = 1216, instr = 'sdi', /load
```

```
plot_image, alog10(oimg), min=0.5, max=4.1, charsize=1.5
xyouts, 150, 150, ohdr.date_obs, charsize=2.
plot_map, sdimap, /log, dmin=40, dmax=14000, charsize=1.5
```

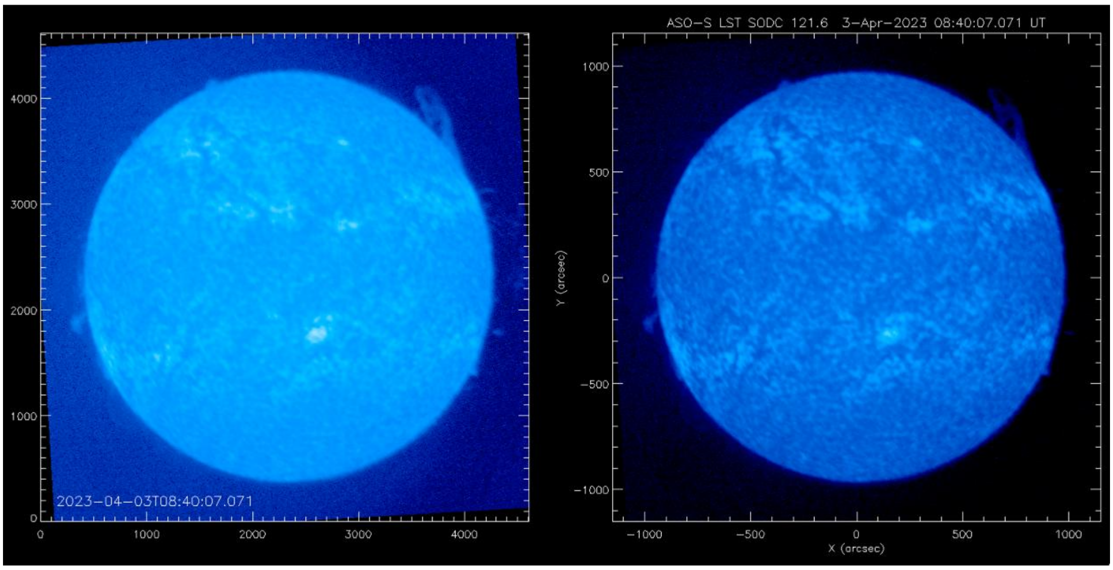


```
index2map, ohdr, oimg, sdimap
sub_map,sdimap,smap, xrange=[500,1100],yrange=[200, 1100]
window, 0, xsize=1600, ysize=800, retain=2
!p.multi=[0,2,1]
lst_lct, wavelnth = 1216, instr = 'sdi', /load
plot_map, sdimap, /log, dmin=10, dmax=14000, charsize=1.5
plot_map, smap, /log, dmin=10, dmax=14000, charsize=1.5
```

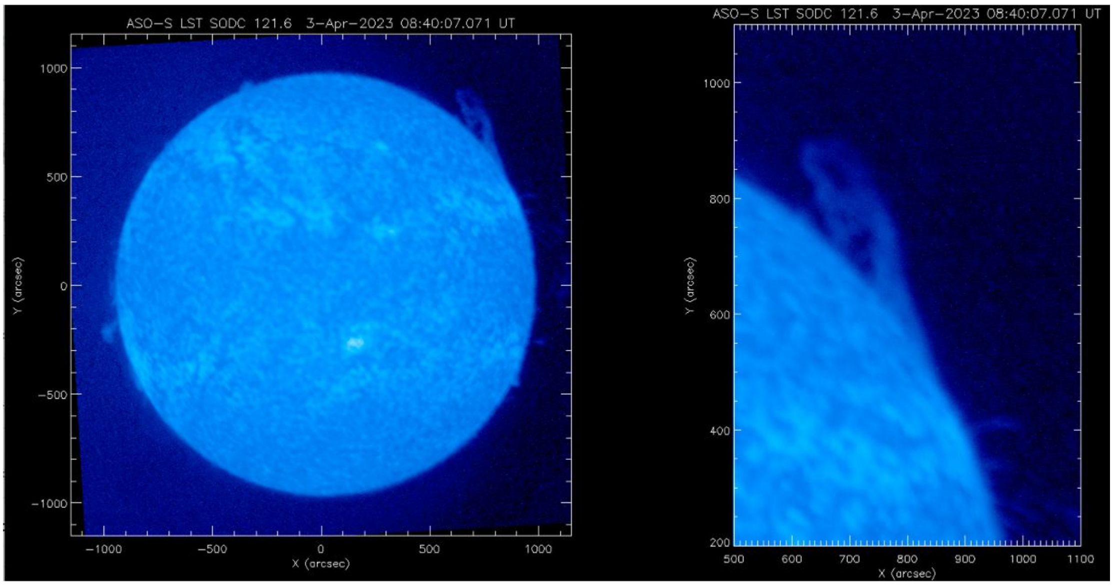

5.3 WST data analysis demo

```
file='/asos/data/wst/science/lev10/2023/04/03/wst_lev10_20230403_235023.595_v01.fits.gz'
read_lst, file, ihdr, iimg
lst_prep, ihdr, iimg, ohdr1, oimg1
lst_prep, ihdr, iimg, ohdr2, oimg2, outsize=4096 ;to work with e.g., SDO/HMI
;lst_prep, ihdr, iimg, ohdr2, oimg2, outsize=4096, /radcalib_on
index2map, ohdr2, oimg2, wstmap
window, 0, xsize=1800, ysize=600, retain=2
!p.multi=[0,3,1]
lst_lct, wavelnth = 3600, instr = 'wst', /load
plot_image, oimg1, dmin=0, dmax=8000, charsize=2., xtitle='X (pixel)', ytitle='Y (pixel)'
plot_image, oimg2, dmin=0, dmax=8000, charsize=2., xtitle='X (pixel)', ytitle='Y (pixel)'
plot_map, wstmap, dmin=0, dmax=8000, charsize=2.
```

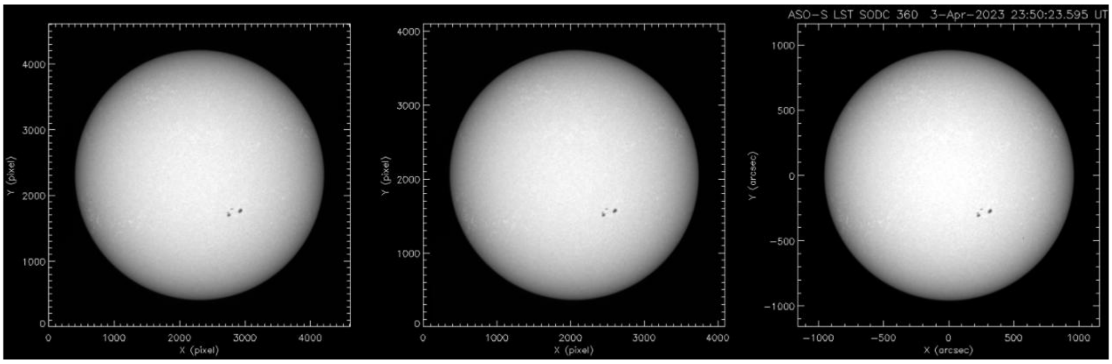

6. References

Gan, W.Q., Zhu. C., Deng, Y.Y., Zhang, Z., Chen, B., Huang, Y., Deng, L., Wu, H.Y., Zhang, H.Y., Li, H., Su, Y., Su, J.T., Feng, L., Wu, J., et al.: The Advanced Space-Based Solar Observatory (ASO-S), 2023, Solar Physics, 298, 68

Li, H., Chen, B., Feng, L., Li, Y., Huang, Y., et al: The Lyman-alpha Solar Telescope (LST) for the ASO-S Mission I. Scientific Objectives and Overview: 2019, Research in Astronomy and Astrophysics, 19, 158

Chen, B., Li, H., …, Feng, L. et al.: The Lyman-alpha Solar Telescope (LST) for the ASO-S Mission II. Design of LST, 2019, Research in Astronomy and Astrophysics, 19,159

Feng, L., Li, H., Chen, B., Li, Y., Susino, R., et al: The Lyman-alpha Solar Telescope (LST) for the ASO-S Mission III. Data and Potential Diagnostics: 2019, Research in Astronomy and Astrophysics, 19, 162

Lu, L., Li, H., Huang, Y., Feng, L., Zhu, B., et al.: The Trigger and Termination Scheme for the event mode of the Lyman-alpha Solar Telescope (LST) onboard the ASO-S Mission, 2020, Chinese Astronomy and Astrophysics, 44, 4, 490-506

Li, J.W., Li, H., Li,Y., Feng, L., et al., In-flight flat field calibration methods for the Lyman-alpha Solar Telescope (LST), 2021, RAA, 21,121

Li, S.T., Feng, L., Li, Y., Li, H., Huang, Y., et al., Synoptic charts in Lyα retrieved from the SDI observations, 2023, Solar Physics, in prep